Fabrication and Phase Transformation in Crystalline Nanoparticles of $PbZrO_3$ Derived By Sol-Gel

Satyendra Singh and S.B. Krupanidhi*

Materials Research Centre, Indian Institute of Science, Bangalore – 560012, India

Abstract: In this research fabrication of crystalline $PbZrO_3$ (PZ) nanoparticles and their phase transformation behavior is investigated. A novel sol-gel method was used for the synthesis of air-stable and precipitate-free diol-based sol of PZ, which was dried at 150 °C and then calcined at 300-700°C for 1 h. The morphology, crystallinity and phase formation of as synthesized nanoparticles were studied by the selected-area electron diffraction (SAED), X-ray diffraction (XRD), thermal gravimetric analysis/differential scanning calorimetry (TGA-DSC), and high resolution transmission electron microscope (HRTEM). The XRD, SAED, and TGA-DSC analyses confirmed the tetragonal lead rich zirconia phase (t-Z phase) and monoclinic zirconia phase (m-Z phase) as the intermediate phases during the calcinations process followed by crystallization of single orthorhombic PZ phase at about 700 °C. The average PZ particle size was observed about 20 nm as confirmed by TEM study. Energy-dispersive X-ray spectroscopy (EDX) analysis demonstrated that stoichiometric $PbZrO_3$ was formed.

Keywords: Nanoparticles, $PbZrO_3$, Sol-gel method, TEM.

INTRODUCTION

Recently, ferroelectric nanomaterials such as nanoparticles, nanotubes and nanowires have taken increasingly important role because of their promising applications in nanoscale piezoelectric actuators and transducers, nonvolatile memory devices, and ultrasonic devices [1-7]. A lot of research has been done on nanoferroelectric devices for memory and other applications [8-11]. Antiferroelectric materials are very promising for a variety of devices, such as sensors, actuators, micromotors, microvalves, micropumps and many other micromechanical devices. Lead zirconate is one kind of antiferroelectric material having a non-permanent electric dipole moment whose complete or partial realignment can be reversed under appropriate conditions. The ferroelectric state can be induced when lead zirconate is subjected to a sufficiently large electric field. This change in bulk material occurs near the Curie point, which is 233 °C for $PbZrO_3$ [12], but in thin films, a typical double hysteresis loop is observed at room temperature [13]. When the applied field is removed a large amount of charge is released [14]. This feature is utilized in many applications such as transducers, charge storage devices, microelectromechanical systems (MEMS) and microsensors [13-16].

In recent years, researchers have focused on synthesizing nanosized PZ particles to improve desired properties utilizing the higher inherent surface area of the nanoparticles for implementation in the microelectronic and microelectromechanical systems [17,18]. In the current work, we have employed a novel sol-gel methodology for the synthesis of air-stable and precipitate-free diol-based sol of PZ to generate crystalline PZ nanoparticles. The phase transformation from intermediate (m-Z and t-Z) phases to orthorhombic phase was investigated as an important aspect of nanoparticles formation.

EXPERIMENTAL

An air-stable and precipitate-free sol of PZ was synthesized by chemical methods based on the diol route [19], whereas 1,3-propanediol, $[HO(CH_2)_3OH]$ and glacial acetic acid $[CH_3COOH]$ were used as solvents, while high purity lead acetate trihydrate $[Pb(CH_3COO)_2.3H_2O$, Aldrich] and zirconium (IV) butoxide solution $[Zr(OC_4H_9)_4$, Aldrich] were used as the precursors. PZ precursor solution was prepared whereby lead acetate was dissolved in 1,3-propanediol and glacial acetic acid with continuous stirring at 70 °C till the complete dissolution of lead acetate then zirconium butoxide was added drop by drop to the solution and stirred at 70 °C for 30 min and the solution was cooled to room temperature. The pH value of the final solution was adjusted to 5-6 by adjusting 1,3-propanediol and glacial acetic acid. The solution, that is usually called PZ precursor solution, was very light yellow and transparent. The PZ sol as prepared was heated on a hot plate whose temperature was increased gradually to 150 °C until a thick sol was formed. The dried gel was grounded to fine powder and further calcined in the furnace at 300 -700 °C/1 h. Finally, light yellow PZ powder was obtained.

The reaction starts with the nucleophilic addition of negatively charged HO− groups on the positively charged metal atom in the transition state. The positively charged proton is then transferred toward an alkoxy group and the protonated RO- ligand is finally removed. The chemical reactivity of metal alkoxides toward hydrolysis and condensation mainly depends on the positive charge of the metal ion and its ability to increase its coordination number [20]. A proposed reaction scheme according to Livage *et al*. [21] is shown in Fig. (**1**). The fine particles were suspended in acetone medium and dropped on to the carbon coated grid. The morphology, selected-area electron diffraction (SAED), structure and composition of the resulting PZ nanoparticles were studied on a transmission electron microscope (TEM, Tecnai F30) equipped with EDX and operated at an accelerating voltage 200 kV. X-ray powder diffraction data were collected on a Philips X'pert pro diffractometer with a copper source. Thermal gravimetric analysis (TGA) and differential scanning calorimetry (DSC) were carried out using a thermal analysis system (TA Instrument) with a heating rate of 10 °C/min over a 30–1000 °C temperature range in the air environment.

RESULTS AND DISCUSSION

The XRD results of PZ precursor gel powder calcined at 300, 450, 550, 600, 650, and 700 °C for 1 h are shown in Fig. (**2**). The precursor gel exhibited amorphous behavior below 300 °C, which indicates that a polymeric network exists holding the metal ions together. The decomposition of lead acetate, and zirconium isopropoxide started above 300 °C. It was observed that PZ was initially crystallized with some intermediate m-Z (monolinic zirconia) and t-Z (tetragonal zirconia) phases [22, 23] at 450-550 °C. The broadness in the peaks may be due to small crystal size. At around 600 °C, these intermediate phases start transforming to orthorhombic phase as several peaks from orthorhombic lattice planes were ob-

*Address correspondence to this author at the Materials Research Centre, Indian Institute of Science, Bangalore – 560012, India; Tel: +91-80-23601330, Fax: +91-80-23607316; E-mails: sbk@mrc.iisc.ernet.in, satyambd@gmail.com

1573-4137/09 $55.00+.00

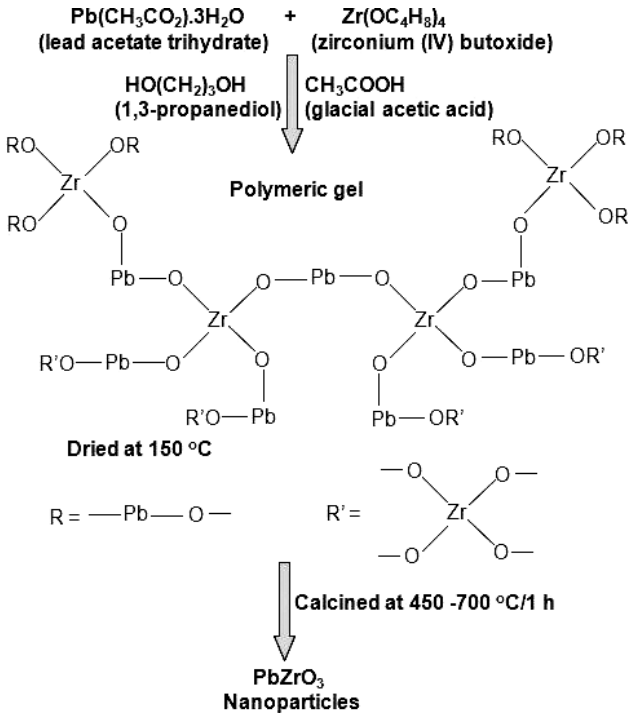

Fig. (1). Proposed reaction scheme for the fabrication of PZ nanoparticles.

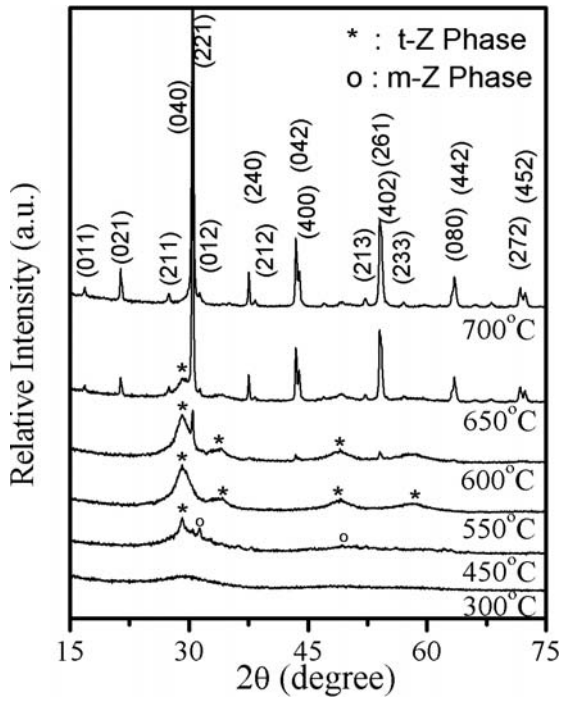

Fig. (2). XRD pattern of PZ gel powder calcined at 300, 450, 550, 600, 650 and 700 °C for 1 h, respectively.

served, as can be seen in Fig. (**2**), which were accompanied by many t-Z peaks, and then finally transformed into pure orthorhombic PZ phase at about 700 °C. The average crystallite size was found to be about 25 nm for the samples annealed 700 °C for 1 h, which was calculated from Scherrer's formula by indexing (221) peak as follows: $T = 0.9\lambda/\beta\cos\theta_B$, where T is the average particle size in angstroms, β is the width of the peak at half the peak height in radians, λ (=1.5406 Å) is the wavelength in angstroms, and θ_B is the Bragg angle in degrees.

Fig. (**3**) shows the thermogram of lead zirconate dried gel powder, obtained from the TGA–DSC technique in the temperature range between 30 and 1000 °C. Total weight loss from room-temperature to 1000 °C of PZ dried gel powder was about 35 %. Only a slight decrease in weight of about 3.5 wt % is observed from 30 to 150 °C, which is attributed to desorption of water, and organic solvents (acetic acid and 1,3 propane diol) present in the powder. The maximum value of weight loss was observed between 240 and 420 °C by exothermic reaction. The weight loss is clearly attributed to the removal of organic species adsorbed to the as-prepared powder particles. The DSC curve indicates that the PZ precursor gel decomposed exothermally with a sharp peak at 404 °C, which is accompanied by two minor peaks at 365 and 280 °C. This sharp peak was directly related to the continuous weight loss observed in the TGA curve and could be associated with the formation of metastable zirconia phases as observed in the XRD. Some minor peaks observed at 365 and 280 °C may be associated with the pyrolysis of propoxy and acetate ligands associated with oxide formation of metal ions. At higher temperature (above 450 °C), no significant weight loss was observed up to 1000 °C, which gives an evidence for the absence of organic residues and proves the stability of the obtained particles at high temperatures, especially regarding the commonly observed PbO loss through evaporation at temperatures above 700 °C.

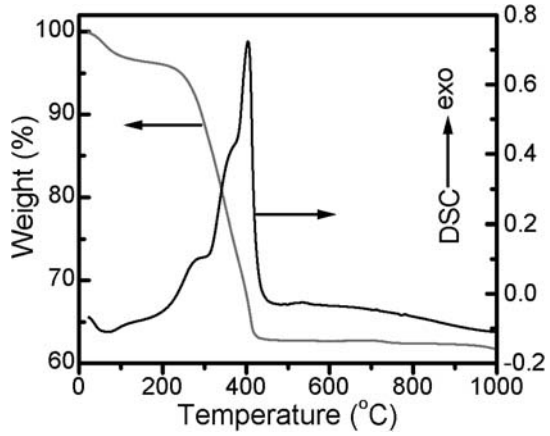

Fig. (3). TGA-DSC curves of PZ dried gel powder.

To study the morphology and detailed microstructure of the resulting PZ powder, two different PZ samples were investigated inside the TEM. First, 550 °C for 1 h calcined PZ precursor powder was subjected to TEM examination. We focused on a small particle on TEM grid and on reaching at higher magnification it revealed numerous tiny nanocrystals inside with size ranging from approximately 3-6 nm, as shown in Fig. (**4a**) and the inset (left top corner) in Fig. (**4a**) shows the corresponding selected area electron diffraction (SAED) pattern. The Circular fine rings in the SAED pattern were identified as intermediate t-Z phase as observed in XRD of this sample (Fig. **2**). The inset (right top corner) in Fig. (**4a**) shows the high-resolution transmission electron microscope (HRTEM) image taken on the isolated nanoparticles present in the PZ precursor powder annealed at 550 °C, which gives further insight into the details of the microstructure of the PZ nanoparticles. The distance between the parallel fringes is about 3.04 Å, corresponding to the well-recognized lattice d-spacing of (111) atomic planes of t-Z phase [22], which agrees well with the values, calculated from the SAED pattern and XRD. Fig. (**4b**) shows TEM image of PZ precursor powder annealed at 700 °C for 1 h and inset (left top corner) shows the corresponding SAED pattern. The average particle size

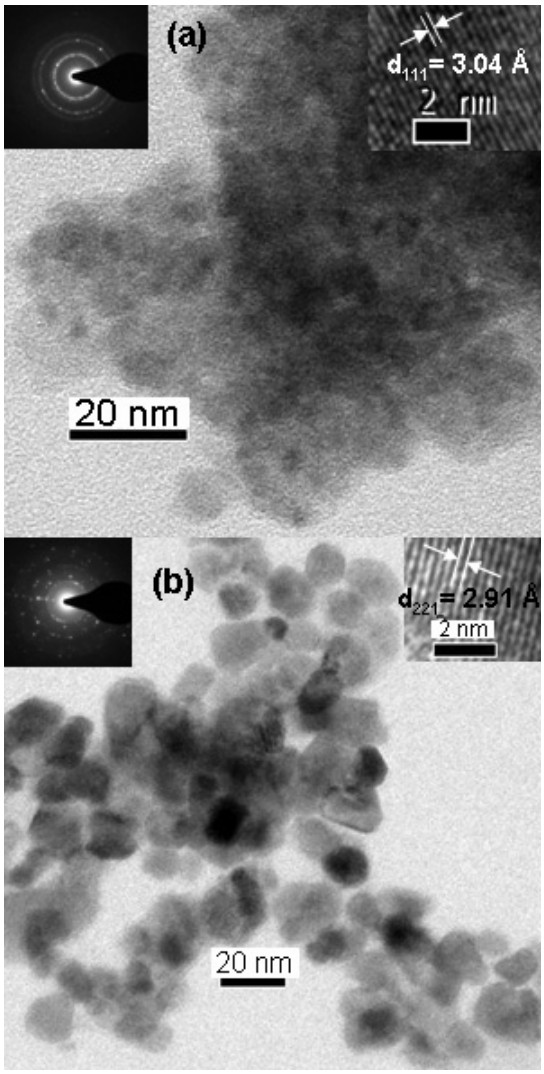

Fig. (4). TEM images: (**a**) PZ gel powder calcined at 550 °C for 1 h and the inset (top left corner) shows the corresponding SAED pattern while inset (top right corner) show the HRTEM image of a PZ nanoparticle. (**b**) PZ gel powder calcined at 700 °C for 1 h and the inset (top left corner) shows the corresponding SAED pattern while inset (top right corner) show the HRTEM image of a PZ nanoparticle.

was about 20 nm and the nanoparticles were nearly freestanding as can be seen in Fig. (**4b**). As expected, increasing the annealing temperature caused the increase in particle size in the samples. SAED patterns clearly show that intermediate phases are transformed into the orthorhombic PZ phase as observed in the XRD analysis. The inset (right top corner) in Fig. (**4b**) shows the HRTEM image taken on the isolated nanoparticles present in the PZ precursor powder annealed at 700 °C for 1 h, which further verified the formation of orthorhombic PZ phase in the PZ nanoparticles. The distance between the parallel fringes is about 2.92 Å, corresponding to the well-recognized lattice d-spacing of (221) atomic planes of orthorhombic PZ phase, which agrees well with the values calculated from the SAED pattern, XRD, and open literature (JCPDS card No. 350739).

In order to determine the chemical composition of as prepared PZ nanoparticles, EDX experiments were performed on individual nanoparticle by the TEM. Only the freestanding isolated nanoparticles were selected in the experiments to avoid effects due to supporting carbon film and other nanoparticles. Fig. (**5**) shows the typical EDX spectra from a PZ nanoparticle. The presence of Pb,

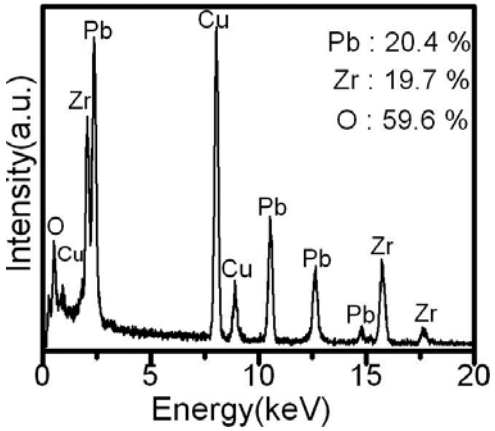

Fig. (5). EDX spectrum from a PZ nanoparticle.

Zr, and O peaks in the spectra indicate that these nanoparticles are made of Pb, Zr, and O with the average atomic ratio Pb : Zr : O :: 0.204 : 0.197 : 0.596, which is very close to the desired composition $PbZrO_3$. The presence of some Cu and C peaks may be attributed to the Cu and carbon coating on TEM grids.

CONCLUSIONS

To summarize, orthorhombic structure PZ nanoparticles were fabricated by a novel sol-gel method based on diol-based solution. Initially, PZ was crystallized with intermediate m-Z and t-Z phases in the temperature range from 400-550 °C and starts transforming to orthorhombic at around 600°C, and then finally transformed into pure orthorhombic PZ phase at about 700 °C. XRD and TEM confirmed the nanocrystalline nature of PZ particles. The lead zirconate nanoparticles produced may have potential applications as materials used in microelectronics and microelectromechanical systems.

REFERENCES

[1] Ahn, H.; Rabe, K. M.; Triscone, J. M. Ferroelectricity at the nanoscale: Local polarization in oxide thin films and heterostructures. *Science*, **2004**, *303*, 488.
[2] Junquera, J.; Ghosez, P. Critical thickness for ferroelectricity in perovskite ultrathin films. *Nature*, **2003**, *422*, 506.
[3] Wang, Y.; Santiago-Aviles, J. J. Synthesis of lead zirconate titanate nanofibres and the Fourier-transform infrared characterization of their metallo-organic decomposition process. *Nanotechnology*, **2004**, *15*, 32.
[4] Luo, Y.; Szafraniak, I.; Zakharov, N. D.; Nagarajan, V.; Steinhart, M.; Wehrspohn, R. B.; Wendorff, J. H.; Ramesh, R.; Alexe, M. Nanoshell tubes of ferroelectric lead zirconate titanate and barium titanate. *Appl. Phys. Lett*., **2003**, *83*, 440.
[5] Chu, M. W.; Szafraniak, I.; Scholz, R.; Harnagea, C.; Hesse, D.; Alexe, M.; Gosele, U. Impact of misfit dislocations on the polarization instability of epitaxial nanostructured ferroelectric perovskites. *Nat. Mater*., **2004**, *3,* 87.
[6] Roelofs, A.; Schneller, I.; Szot, K.; Waser, R. Piezoresponse force microscopy of lead titanate nanograins possibly reaching the limit of ferroelectricity. *Appl. Phys. Lett.,* **2002**, *81*, 5231.
[7] Scott, J. F.; de Araujo, C. A. P. Ferroelectric memories. *Science*, **1989**, *246,* 1400.
[8] Scott, J. F.; Alexe, M.; Zakharov, N. D.; Pignolet, A.; Curran, C.; Hesse, D. NANO-phase SBT-family ferroelectric memories. *Integr. Ferroelectr*., **1998**, *21*, 1.
[9] Scott, J. F. [3D] Nano-scale ferroelectric devices for memory applications. *Ferroelectrics*, **2005**, *314*, 207.
[10] Gruverman, A.; Kholkin, A. Nanoscale ferroelectrics: processing, characterization and future trends. *Rep. Prog. Phys.,* **2006**, *69*, 2443.
[11] Scott, J. F.; Morrison, F. D.; Miyake, M.; Zubko, P. Nano-ferroelectric materials and devices. *Ferroelectrics*, **2006**, *336*, 237.
[12] Shirane, G.; Sawaguchi, E.; Takagi, Y. Dielectric properties of lead zirconate. *Phys. Rev*., **1951**, *84*, 476.
[13] Bharadwaja, S.S.N.; Krupanidhi, S. B. Dielectric relaxation in antiferroelectric multigrain $PbZrO_3$ thin films. *Mater. Sci. Eng. B*, **2000**, *78*, 75.
[14] Bharadwaja, S.S.N.; Saha, S.; Bhattacharyya, S.; Krupanidhi, S. B. Dielectric properties of La-modified antiferroelectric $PbZrO_3$ thin films. *Mater. Sci. Eng. B*, **2002**, *88*, 22.
[15] Tang, X.G.; Wang, J.; Wang, X. X.; Chan, H.L.W. Electrical properties of highly (111)-oriented lead zirconate thin films. *Solid State Commun*., **2004**,

130, 373.

[16] Tang, Z.; Tang, X. Structural, dielectric and optical properties of highly oriented lead zirconate thin films prepared by sol–gel process. *Mater. Chem. Phys.,* **2003**, *80,* 294.

[17] Yamakawa, K.; Trolier-McKinstry, S.; Dougherty, J.P.; Krupanidhi, S. B. Reactive magnetron co-sputtered antiferroelectric lead zirconate thin films. *Appl. Phys. Lett*., **1995**, *67*, 2014.

[18] Ayyub, P.; Chattopadhyay, S.; Sheshadri, K.; Lahiri, R. The nature of ferroelectric order in finite systems. *NanoStruct. Mater.,* **1999**, *12*, 713.

[19] Calzada, M. L.; Alguero, M.; Ricote, J. Santos, A.; Pardo, L. Preliminary results on sol-gel processing of 100 oriented $Pb(Mg_{1/3}Nb_{2/3})O_3$-$PbTiO_3$ thin films using diol-based solutions. *J. Sol-Gel Sci. Techn*., **2007**, *42*, 331.

[20] Livage, J.; Sanchez, C.; Babonneau, F. In: *Chemistry of Advanced Materials An Overview* Ch. 9. Iterrante, L.V.; Hampde-Smith, M.J., Eds.; Chem Adv Mater, Wiley-VCH: New York, **1998**, p. 389.

[21] Livage, J.; Henry, M.; Sanchez, C. Sol-gel chemistry of transition metal oxides. *Prog. Solid State Chem*., **1988**, *18*, 259.

[22] Ko, T.; Hwang, D. K. Preparation of nanocrystalline lead zirconate powder by homogeneous precipitation using hydrogen peroxide and urea. *Mater. Letts.,* **2003**, *57*, 2472.

[23] Camargo, E. R.; Popa, M. Frantti, J.; Kakihana, M. Wet-chemical route for the preparation of lead zirconate: an amorphous carbon- and halide-free precursor synthesized by the hydrogen peroxide based route. *Chem. Mater.,* **2001**, *13*, 3943.

Received: December 28, 2008 Revised: May 05, 2009 Accepted: May 23, 2009